Hydraulic Failure and soil-structure deformation due to wave and draw down loading

M. Davis[1], H.-J. Köhler[2], M.A. Koenders[1] & R. Schwab[2]

Abstract In engineering practice submerged soils are commonly considered to be saturated and consequently the pore fluid may be regarded as incompressible. At shallow water depths this two-phase model is not in accordance with natural conditions. Even small quantities of gas bubbles change the stiffness properties of the pore fluid dramatically. In response to external fluctuating pressures, the gas bubbles in the pores experience a volume change, thus causing local transient flow. The latter must be consistent with the permeability law of the soil. Based on Biot's consolidation equation, both uncoupled and coupled numerical simulations and analytical estimates have been employed, demonstrating that time-varying pressure loading contributes to soil deformation, fluidization and hydraulic failure. A variety of geotechnical situations is reviewed. These include rapid draw-down, wave loading and turbulent water current acting on both a protected or unprotected sandy soil bed in shallow water. The actual pore pressure response of the submerged subsoil has been calculated. It is demonstrated that this loading contributes to sand bed deformation, fluidization and associated failure. The vulnerability to erosion and scouring is emphasised.

Introduction

It is well-known that the constitutive properties of soil depend on the degree of saturation of the water that occupies the interstices of the grain matrix: Fredlund and Rahardjo (1993). A report on – for example – the influence of the degree of saturation, S, on the Critical-state parameters of a sample of soil is given in a recent paper by Toll and Ong (2003) and further in the references provided by these authors. It is clear from this body of research that the mechanical properties vary smoothly with the volume fraction of the gas (in bubble form) in the fluid, so that for nearly saturated conditions the constitutive properties can be obtained entirely from the effective stress as estimated by Terzaghi's stress principle. For near-saturated conditions, however, the pore water may be substantially more compressible than the skeletal matrix. For example, for a saturation of some 95% the compressibility of the pore water at atmospheric pressure may be estimated as (see Bishop and Eldin (1950)) $5\times10^{-7}\,Pa^{-1}$, compared to a value of $10^{-8}-10^{-9}\,Pa^{-1}$ for a dense sand. Saturated water has a compressibility of $4.6\times10^{-10}\,Pa^{-1}$; this value is so low that in many applications the fluid may be considered to be incompressible compared to the soil matrix. A small amount of gas has a large impact on the stiffness of the fluid. In

[1] Department of Mathematics, Kingston University, Penrhyn Road, Kingston on Thames, Surrey, KT1 2EE, UK; mast@kingston.ac.uk or koenders@kingston.ac.uk
[2] Abt. Geotechnik, Bundesanstalt für Wasserbau, Kussmaulstrasse 17, 76138 Karlsruhe, Federal Waterways Engineering and Research Institute, Geotechnical Department, Karlsruhe, Germany, koehler@baw.de or schwab@baw.de

any geotechnical situation in which the process involves a deformation of both the fluid and the skeletal matrix together, the degree of saturation – though it may be small – needs to be known to predict the deformation and flow fields correctly. At the same time the amounts of gas are so small that the constitutive properties of the soil remain virtually unaffected.

Below a number of geotechnical applications are outlined in which the compressibility of the fluid plays a vital role. Typically these applications are concerned with the prediction of erosion due to soil fluidization. They may take place at the surface of a sea bed or inland waterway and are due to an external pressure variation caused by waves (which in turn may be caused by shipping movement) or by fast draw down – for example in a lock.

In the past the authors have developed a simple formula based on a one-dimensional solution of Biot's equation (Biot (1941)), which permits an estimate of the critical factors that affect a possible fluidization process: Köhler and Koenders (2003). This estimate is based on an unprotected boundary between soil and water, that is, no top load has been applied to increase the skeleton stress. The factors that are involved are: (1) the water depth of the soil/water boundary y_0, (2) the rate at which the external pressure drops $\bar{\sigma}$, (3) the duration of the pressure drop t_0, (4) the saturation of the fluid in the subsoil *S*, (4) the porosity of the subsoil *n* and (5) the permeability of the soil *k*. The formula evaluates a 'critical time' t_1, expressed in Terzaghi's critical gradient of the soil i_c and the unit weight of water γ_w

$$t_1 = \frac{\pi}{4} y_0 \left(\frac{i_c \gamma_w}{\bar{\sigma}} \right)^2 \frac{k}{n(1-S)} \qquad (1)$$

No fluidization occurs when $t_0 < t_1$; the moment of onset of fluidization is t_1, which is the point at which the skeletal stress vanishes at the top of the soil. The criterion for fluidization is Terzaghi's criterion: if the pressure gradient exceeds the weight of the soil, then the bed fluidizes.

The formula forms the ratio of a group of soil property parameters $k/[n(1-S)]$, which have the dimension of a velocity, with a group of external loading parameters $\frac{4}{\pi} t_0 (\bar{\sigma} / i_c \gamma_w)^2 / y_0$, which also has the dimension of a velocity. If the velocity associated with the soil properties is less than the velocity associated with the external loading then fluidization occurs. In that case the soil cannot respond quickly enough to the loading that is introduced by the external pressure drop. Once fluidization takes place the soil is vulnerable to erosion associated with a simultaneous horizontal flow. For fluidized soils only a small horizontal flow is required to effect transport of the grains. Calculation of the amount of transported material is possible for beds for which no internal fluidization is present: Jenkins and Hanes (1998) developed the sheet flow calculation. This calculation has not yet been extended to include a simultaneous vertical flow.

Formula (1) is an estimate, valid for one dimensional situations in which the compressibility of the water is substantially greater than the compressibility of the

soil skeleton, while the soil surface is unprotected and the external pressure drop is a steady one. Modifications to all these conditions can be introduced. Especially the presence of the top load, the thickness and grainsize of which may be designed, is worth investigating and the result of such an inquiry has been reported by Roussell *et al* (2000).
Formula (1) is a theoretical prediction. In an effort to measure subsoil fluidization effects and verify Formula (1) in a controlled environment, an endoscopic technique has been developed. The results of this research have been reported by Koehler and Koenders (2003) and the expression has been found to be correct.

Fluidization due to draw-down loading for a top-loaded sandy soil

The scenario of a partially saturated sandy soil that is protected by a top load that consists of gravel is illustrated. The sea bed is assumed to be at a water depth of 10 *m*; the protective gravel layer has a thickness of 10 *cm*. The gravel has been introduced to prevent current-induced soil erosion.

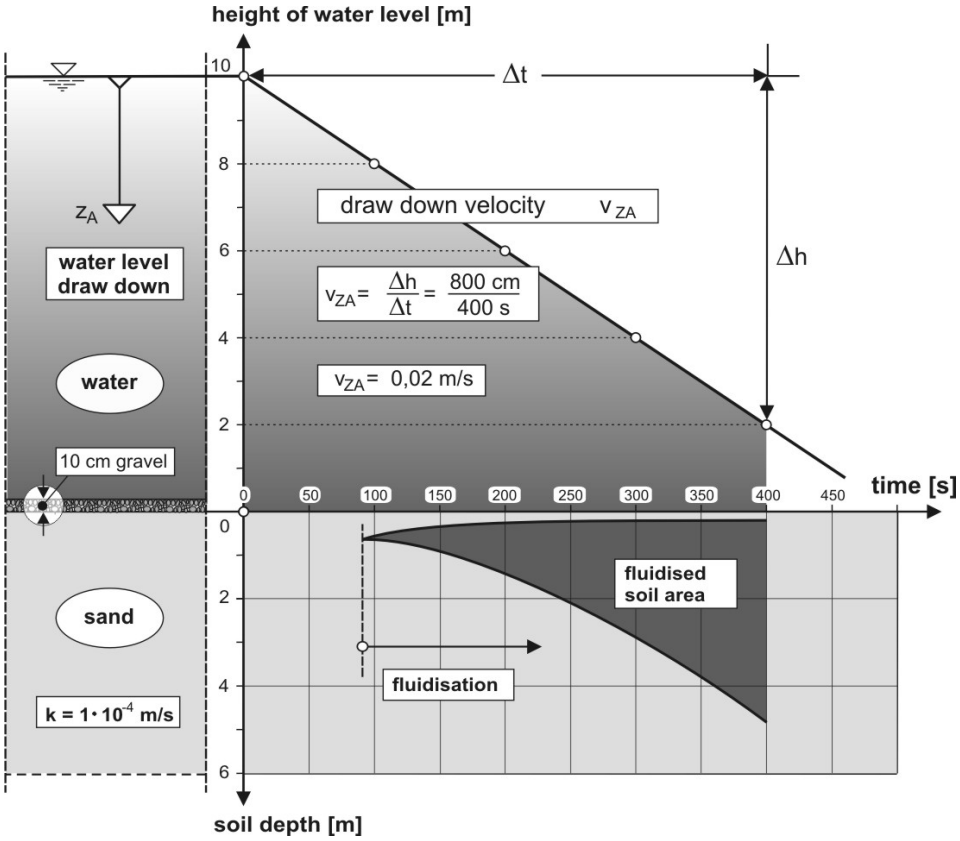

Figure 1. Illustration of the temporal extension of the fluidized zone for the case of a top load protected sand under an external pressure drop.

In the case of protected soil the fluidization does not start at the top of the layer, but there is a zone in which the skeletal stress is smaller than the weight of the soil. This

zone is illustrated in Figure 1. Just as in the case of the unprotected bed the duration of the draw-down is important, though it is not possible to express the problem in simple analytical formulas, such as Formula (1). The analysis for the top load protected case has been reported by Roussell *et al* (2000).

In the illustration given in Figure (1) the sand has a permeability k of $1.\times 10^{-4}\ m/s$; the external water level falls at a rate of $0.02\ m/s$. The fluidization commences after some 90 seconds. The fluidized zone extends rapidly as a function of time while the draw-down continues. The top of the zone never quite reaches the top of the sand-gravel interface, while the lower bound of the zone continues to extend deeper as the external pressure is decreased.

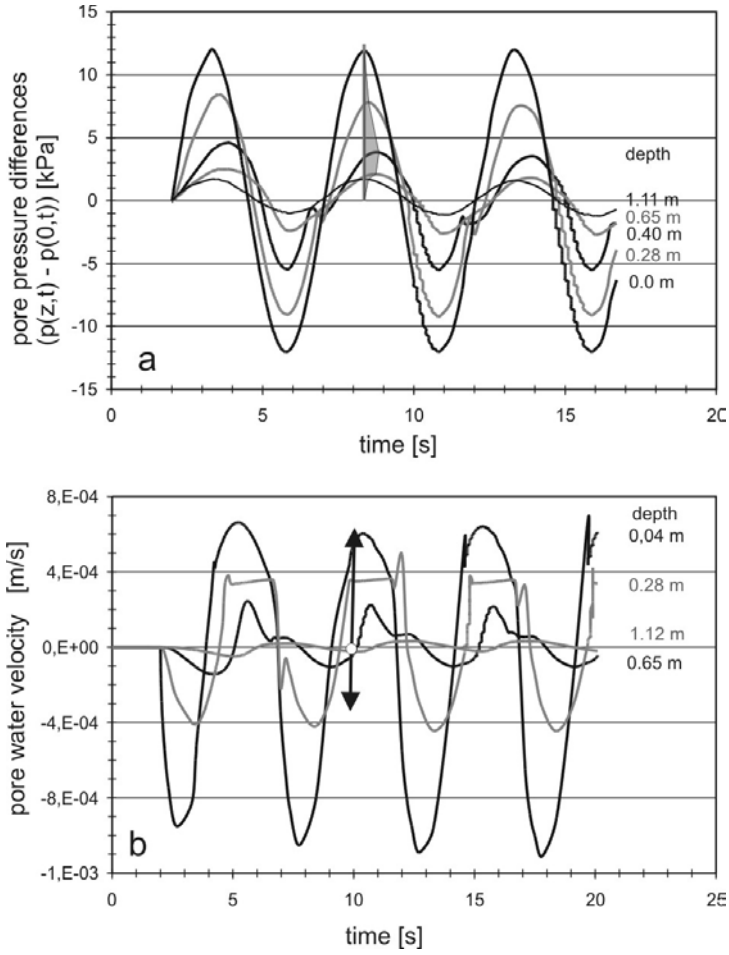

Figure 2. (a) Excess pore pressures and (b) pore water velocities as a function of time and depth for a one-dimensional solution of a wave loaded subsoil.

If no top load is present, the fluidization takes place at an earlier point and commences at the water-sand interface. Thus, the application of top load assists in avoiding damage by postponing the point at which fluidization sets in so that external

pressure drops of greater duration can be accommodated without the risk of fluidization.

Fluidization due to wave loading (one dimensional solution)

Possible soil bed deformations in an unsaturated submerged soil may be caused by external pressure changes. In this section the case of cyclic loading is considered. The details of the calculation are reported in Schwab *et al*. (2003).

Heaving, settling and fluidization of the sand bed may take place, causing deformation of the grain skeleton and soil failure. Figure 2 shows the results of the computed pore pressure response and the induced pore water velocities at different depth levels in a 2 *m* thick soil bed, induced by a sinusoidal wave loading acting on a shallow sea bed at 4 *m* water depth. The material of the soil bed consists of uniform sand with a permeability of $k = 2.5 \times 10^{-5}\ m/s$. The wave has a period of 5 *s* and a wave height of 2.4 *m*.

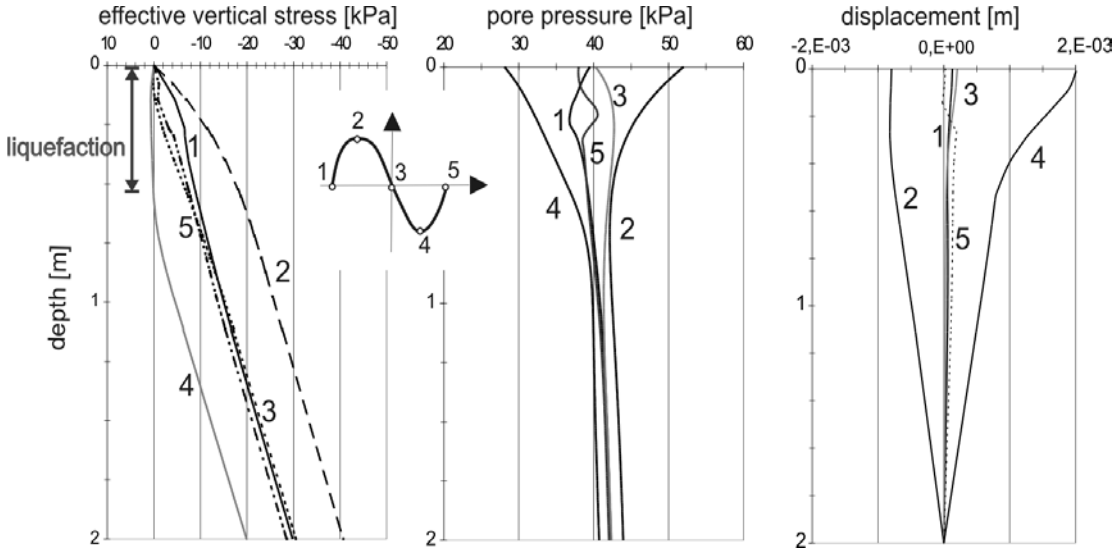

Figure 3. Skeleton stress, pore pressure and soil displacement as a function of depth for various times for a one-dimensional solution of a wave loaded subsoil.

The calculation shows that there is a phase shift between the applied wave and the response in terms of the pore water velocity and excess pressure. Also, the amplitude of the wave is damped as it travels into the soil. Distinct non-linearities are observed as the external pressure (associated with the instantaneous wave height) falls; these

are due to fluidization: while the soil is in this state the pressure gradient cannot increase beyond the critical value. Note that while part of the soil is in a fluidized state, there are other parts where the velocity of the pore water is actually directed downwards. These phase shifts are further illustrated in Figure 2b.
The effective vertical stress, pore pressure and displacement as a function of depth are presented in Figure 3 at different loading stages. The depth of the liquefied strata is restricted to the upper soil layers: less than 0.5 *m* at loading stage 2. The pore pressure distribution is still disturbed by fluidization, even in the neutral loading stages 1, 3 and 5. As expected, larger displacements occur in the regions where the soil is liquefied. The depth of the fluidized soil area is marked in Figure 3: it is seen that the extent of this region comes to some 0.5 *m* below the seabed for the parameters chosen in this illustration.

Fluidization due to travelling waves (two dimensional solution)

In the one-dimensional calculation in the previous Section the influence of horizontal soil displacements caused by the propagation of waves has been neglected. In order to evaluate these effects a two-dimensional analysis has been performed. The same wave characteristics as before have been used, but in addition the wave is given a velocity of 5 *m/s*. The result is plotted in Figure 4.

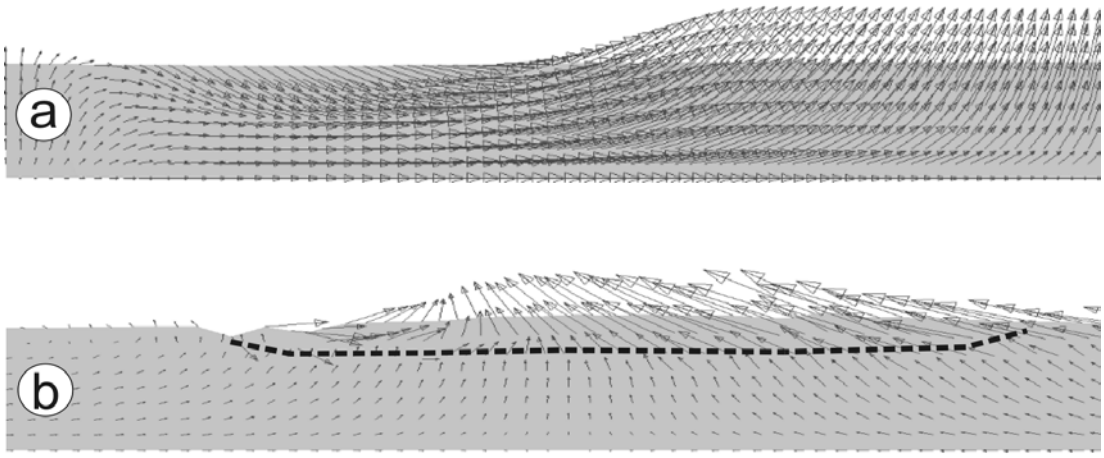

Figure 4. Displacement fields using an elastic soil model (a) and a viscous model for the fluidized soil (b) in a two dimensional finite element simulation of wave loading with travelling wave.

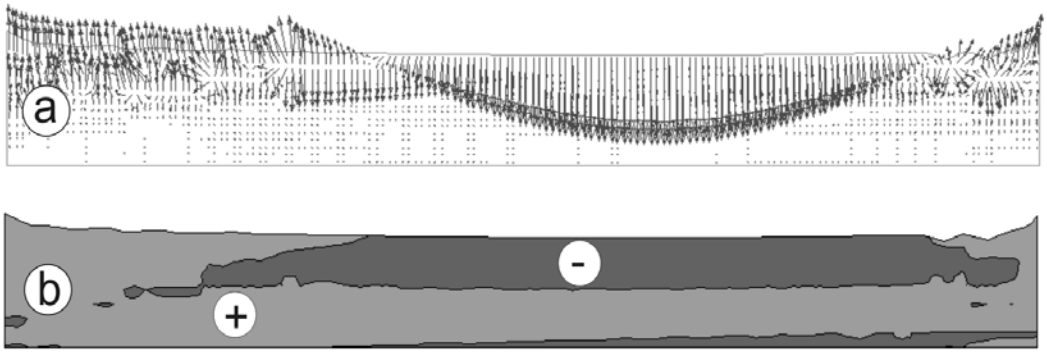

Figure 5. (a) Pore water velocity field for travelling wave loading. (b) Areas with either upward (+) or downward (-) pointing pore water velocities.

This two-dimensional calculation is more involved than the one-dimensional ones. A finite element scheme has been used to gain insight in the possible solutions; the details of the methodology are reported in Schwab *et al*. (2003). The soil model has two possible states: solid or fluidized. The liquefaction takes place where the vertical water pressure gradient exceeds the unit weight of the soil. As the liquefaction represents a stress-softening process there are instabilities associated with this state in a finite element simulation: Bardet (1996). In order to have some control over the numerical instabilities an explicit procedure with variable time-step has been implemented.

Figure 4 describes the displacement fields for two models: in the first model, (a), linear elastic soil behaviour has been adopted. In the second model, (b), the soil behaves viscously as fluidization occurs.

As expected, in the case when the liquefaction takes place (Fig. 4b), the soil particle trajectories do not return to their origin after one cycle. The amplitude of the motion is up to four times larger than in the elastic soil case and is directed against the motion of the propagating wave.

An interesting result of the simulations is presented in Figure 5. In the upper figure part (a) a snapshot of the pore water velocity field is shown and in the lower part (b) the associated flow direction is indicated. In this figure the snapshot time is chosen in such a way that the rising part of the travelling wave is on the right-hand side of the picture, while the left-hand side shows liquefaction due to the action of the falling part of the wave. In the loading domain the water flow is converging due to the superposition of two simultaneously acting flows. The retardant, upwardly directed flow at greater depth caused by the preceding falling wave is countered by the downward flow caused by the rising wave part that takes place simultaneously.

In the liquefied zone a divergent water flow can be observed. The water in the upper part is already moving upwards, whilst in the lower part the flow remains directed

downwardly. The borderline between these two modes of motion indicates the edge of the liquefied zone. In each cycle the effective stress is substantially reduced by the wave loading, causing transient excess pore pressures in which soil particle transport may easily be induced. Due to the loss of inter-granular friction, while the soil is liquefied, enhanced erosion of the soil bed may be observed when a simultaneous horizontal current is present. Transients and bed deformations, such as the development of sand ripples, will take place at the sea bed, recent theory to describe this has been developed by, for example, Hoyle and Woods (1997).

Turbulent current acting on a protected or unprotected river bed (lattice Boltzman Simulation)

Flow is considered over an obstacle placed on a coarse gravel layer that covers a sand layer. The pressure distribution as a function of position and time is obtained for partially saturated conditions in the subsoil. The flow in the open water and coarse layer is calculated using a lattice Boltzmann technique; the pressure in the subsoil is evaluated by means of an analytical solution using the lattice Boltzmann simulation as boundary condition. This is an example of a calculation in which the geometry and the resulting flow features are highly complex (see Figure 6), but by combining the lattice-Boltzmann technique with the analytical technique (specialised towards unsaturated conditions) an appropriate way of modelling the whole system has been obtained.
The results demonstrate where the greatest risk of damage to the subsoil may be located. Various extensions include parameter sensitivity studies. Insofar as the subsoil is concerned, these may be carried out with relative ease, because the same lattice Boltzmann simulation boundary condition results can be used to study the pore pressure response.

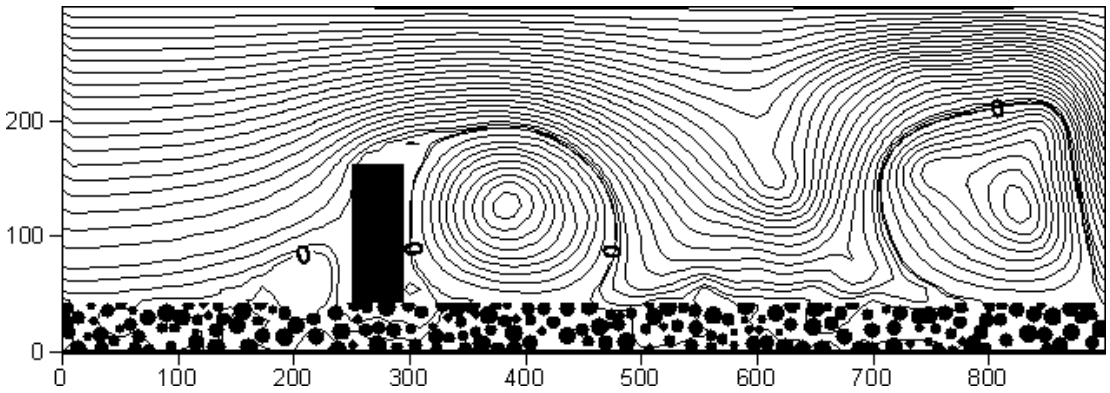

Figure 6. Snapshot of the flow lines as a function of the position for the case of flow over an obstacle.

In essence, the velocity variations due to turbulence cause fluctuations in the pressure on the soil-gravel interface. Where these are falling pressures damage may occur. The calculation method therefore gives an impression of the location where damage

is most likely to occur. The details of the calculation are reported in Davis *et al* (2003).

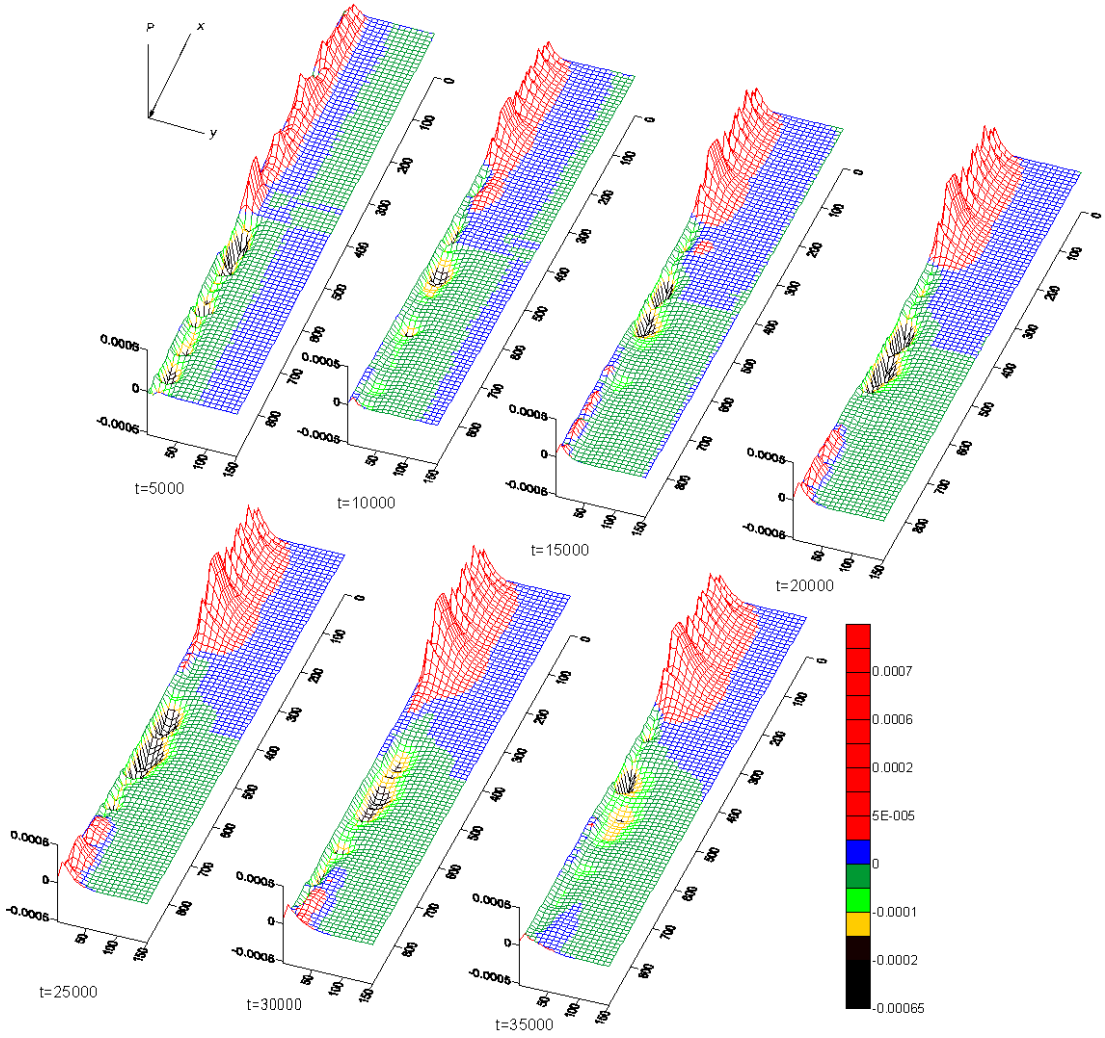

Figure 7. Illustration of a sequence of excess pore pressure profiles at different times for fully developed turbulence. Direction of flow is the x-axis, y-axis is depth of sand and P is the pressure inside the sand.

In order to ascertain erosion sensitivity the direction of the excess pore pressure gradient is important. The illustration in Figure 7 shows that the region that is most prone to a rate of change of pore pressure variation is behind the obstacle. Here the pore pressure gradient oscillates with the passing of the rolling eddies. The results obviously depend on the choice of the parameters of the problem. For conditions that are relevant to model testing with a rectangular obstacle it is shown that the excess pore pressure variations in the subsoil vary with time, making a region behind the obstacle vulnerable to erosion damage.

Conclusions

The effect of small amounts (<10%) of gas in bubble form in pore water in subsoil in shallow conditions is to make the pore water highly compressible compared to the stiffness of the soil skeleton. The effect associated with this phenomenon during external pressure drop is to make the soil vulnerable to liquefaction. Various practical geometries are discussed to demonstrate calculation techniques to indicate at what point and under what circumstances soil fluidization may take place. The geometries that are reviewed are one-dimensional draw-down loading of a sand with and without a permeable gravel protection, one-dimensional and travelling wave loading over an unprotected sand layer and turbulent loading (generated by flow over an obstacle) over a protected sand layer.

Acknowledgement

MAK gratefully acknowledges the use of facilities at the Isaac Newton Institute, Cambridge during the autumn of 2003.

References

Bardet, J.P. (1996) "Scaled memory description of hysteretic material behavior." *J. Appl. Mech.* **63** (3): 750-757.

Bardet, J.P. (1996) "Finite element analysis of two-phase instability for saturated porous hypoelastic solids." *Engineering Computation,* **13** (7): 29-48.

Biot M.A. (1941) "General theory of three dimensional consolidation." *J. Appl. Physics*, **12**: 155-164.

Bishop, A.W. and Eldin, A.K.G. (1950) "Undrained triaxial tests on saturated sands and their significance in the general theory of shear strength." *Géotechnique,* **2** (1): 13-32.

Davis M., Köhler H.J. and Koenders M.A. (2003) "Unsaturated subsoil erosion protection in turbulent flow conditions". Submitted. *Journal of Hydraulic Research (IAHR)*

Fredlund D.G. and Rahardjo H. (1993) *Soil mechanics for unsaturated soils*. New York, Wiley.

Hoyle RB & Woods A.W. (1997) "Analytical model of propagating sand ripples." *Phys Rev E* **56** (6), 6861-6868.

Jenkins J.T, Hanes D.M. (1998) "Collisional sheet flows of sediment driven by a turbulent fluid." *J. Fluid Mech* **370**: 29-52

Köhler, H. J. & Koenders, M. A. (2003) "Direct visualisation of under water phenomena in soil-fluid interaction and analysis of the effect of an ambient pressure drop on unsaturated media." *Journal of Hydraulic Research (IAHR)* **41** (1): 69-78.

Roussell, N., Köhler, H. J. & Koenders, M. A. (2000) "Analysis of erosion protection measures in partially saturated subsoil." *Filters and Drainages in Geotechnical and Environmental Engineering, Proceedings of the 3rd International Conference Geofilters*, Warsaw, Poland, (eds. W. Wolski *et al*.), Rotterdam, A. A. Balkema: 75-81.

Schwab, R. & Köhler, H. J. (2003) "Behaviour of near-saturated soils under cyclic wave loading." *Proceedings of the Third International Symposium on Deformation Characteristics of Geomaterials (IS Lyon 2003)*, Lyon, France, (eds. Di Benedetto *et al*.), A.A. Balkema Publishers, Lisse: 857-862.

Toll D.G. and Ong B.H. (2003) "Critical-state parameters for an unsaturated residual sandy clay". *Géotechnique* **53** (1): 93-103.